Available online at www.sciencedirect.com
SCIENCE DIRECT
Journal of Molecular Catalysis A: Chemical 247 (2006) 80–87
JOURNAL OF MOLECULAR CATALYSIS A: CHEMICAL
www.elsevier.com/locate/molcata

Vapour phase hydrogenation of cinnamaldehyde over silica supported transition metal-based bimetallic catalysts

Benjaram M. Reddy [a,*], Gundapaneni M. Kumar [a], Ibram Ganesh [b], Ataullah Khan [a]

[a] *Inorganic and Physical Chemistry Division, Indian Institute of Chemical Technology, Uppal Road, Hyderabad 500007, India*
[b] *Ceramic Materials Division, International Advanced Research Centre for Powder Metallurgy and New Materials (ARCI), Balapur (PO), Hyderabad 500005, India*

Received 22 September 2005; received in revised form 10 November 2005; accepted 16 November 2005
Available online 22 December 2005

Abstract

A series of silica supported transition metal-based bimetallic catalysts M–M^1/SiO_2 (M = Co, Ni, and Cu; M^1 = Ni, Cu, and Co) were prepared by deposition–precipitation method. Nitrate salts of the corresponding transition metals and colloidal silica were used as the precursors. The physicochemical characteristics of the prepared catalysts were investigated by means of X-ray powder diffraction, thermogravimetry, FT-infrared, scanning electron microscopy-energy dispersive X-ray analysis, and BET surface area techniques. These catalysts were evaluated for selective hydrogenation of cinnamaldehyde to cinnamyl alcohol in the vapour phase at normal atmospheric pressure. Among the various catalysts investigated, the Cu–Co/SiO_2 combination catalyst exhibited very promising results for the selective hydrogenation of cinnamaldehyde to cinnamyl alcohol, whereas Co–Ni/SiO_2 and Ni–Cu/SiO_2 bimetallic catalysts provided good yields of hydrocinnamaldehyde.

Keywords: Bimetallic catalysts; Co–Ni/SiO_2; Ni–Cu/SiO_2; Cu–Co/SiO_2; Selective hydrogenation; Cinnamaldehyde; Cinnamyl alcohol; Hydrocinnamaldehyde

1. Introduction

Research in heterogeneous catalysis is increasingly focused on the chemo- and regio-selective catalytic hydrogenation of α,β-unsaturated carbonyl compounds to produce fine chemicals [1,2]. The selective hydrogenation of α,β-unsaturated carbonyls is a key step in the manufacture of pharmaceuticals, flavors and fragrances [3–7]. The hydrogenation of C=C bond to yield saturated carbonyls is thermodynamically favored and can be readily achieved with high selectivity. However, the selective hydrogenation of C=O bond to provide unsaturated alcohols is much more difficult to achieve [3]. Cinnamaldehyde selective hydrogenation is one such important commercial reaction, which gives cinnamyl alcohol, hydrocinnamaldehyde and phenyl propanol as products. Cinnamyl alcohol is a valuable chemical in the perfumery industry for its odour and fixative properties. It is, also, used as an intermediate in the pharmaceuticals for the synthesis of antibiotic-chloromycetin [8,9]. Recently, hydrocinnamaldehyde has been found to be an important intermediate in the preparation of pharmaceuticals used in the treatment of HIV [10,11]. Although various attempts have been made in the literature to develop a suitable catalytic system for selective hydrogenation of cinnmaldehyde to cinnamyl alcohol or hydrocinnamaldehyde, the selectivity is still an important issue [12,13]. Industrial relevance of unsaturated alcohols in conjunction with economically constraining methods based on chemical reduction of unsaturated carbonyl compounds calls for the development of new catalysts for selective preparation of unsaturated alcohols [14].

A few articles can be found in the literature on the use of group VIII metals deposited over oxidic supports for selective hydrogenation of α,β-unsaturated aldehydes [3,15–17]. Conventional catalysts based on metals such as nickel, palladium or rhodium are almost unselective towards unsaturated alcohols [3]. Although, ruthenium itself is just moderately selective, and similar or better selectivities can be achieved with osmium, iridium or platinum catalysts [18]. Palladium catalyst is known to be effective for the selective hydrogenation of α,β-unsaturated aldehydes to saturated aldehydes. However, such selective reactions are quite problematic when the carbon–carbon double bond

* Corresponding author. Tel.: +91 40 27160123; fax: +91 40 27160921.
E-mail addresses: bmreddy@iict.res.in, mreddyb@yahoo.com (B.M. Reddy).

1381-1169/$ – see front matter © 2005 Elsevier B.V. All rights reserved.
doi:10.1016/j.molcata.2005.11.026

of an unsaturated aldehyde is conjugated both to a carbonyl group and an aromatic ring [12,19]. The high costs of precious metals, their limited availability, sensitivity to sulfur poisoning, and the decrease of selectivity at high temperatures have long been motivated the search for better substitute catalysts [20]. Additionally, it was found that the catalyst deactivation rate in monometallic catalysts is significant and hence the low stability predominates [21]. Therefore, in the field of hydrogenation bimetallic catalysts are often used in order to improve selectivity and stability of a single component catalyst [22].

In general, supported bimetallic catalysts are very interesting materials because one metal can tune and/or modify the catalytic properties of the other metal as a result of both electronic and structural effects [22]. Bimetallic catalysts supported on high surface area carriers, such as, silica and alumina, have attracted considerable attention recently because of their better performance in catalytic reactions which differs significantly from that of the corresponding monometallic counterparts [21]. Additionally, the preparation of supported bimetallic catalysts (by deposition–precipitation) may lead to catalysts with new characteristics, where a specific interaction between the two metals could produce a hybrid catalyst whose behavior may differ from that of the catalysts prepared by conventional methods. In order to achieve absolute selectivity towards unsaturated alcohols, the promotion of either the C=O double-bond polarization and/or the inhibition of the α,β-unsaturated aldehyde adsorption through the C=C bond is necessary and this could be achieved by the presence of two metals in a given catalytic system. So far several reports have appeared on the liquid phase hydrogenation of cinnamaldehyde under different reaction conditions [6–22]. Nevertheless, a few studies have been realized in the gas phase with well-defined metal surfaces. Hydrogenation of crotonaldehyde and methyl crotonaldehyde (prenal) have been studied over Pt(1 1 1) and PtFe(1 1 1) single crystals [23,24]. However, no such attempts can be found in the literature on the vapour phase hydrogenation of cinnamaldehyde. In the present study, a series of transition metal-based bimetallic M–M^1/SiO_2 (M = Co, Ni, and Cu; M^1 = Ni, Cu, and Co) catalysts were prepared by deposition–precipitation method, characterized by TGA, BET SA, XRD, FT-IR and SEM-EDX techniques, and evaluated for hydrogenation of cinnamaldehyde to cinnamyl alcohol in the vapour phase at normal atmospheric pressure.

2. Experimental

2.1. Catalyst preparation

A series of silica supported transition metal-based bimetallic catalysts M–M^1/SiO_2 (M = Co, Ni, Cu and M^1 = Ni, Cu, Co) were prepared by deposition–precipitation method. Both the metals (M–M^1) were loaded in 1:1 mole ratio (based on metals) keeping the loading amount constant at 20 wt.% w.r.t. SiO_2. In a typical preparation, the requisite quantities of the respective nitrate precursor salts were dissolved in deionized water and mixed together. To this mixture solution, required quantity of colloidal silica was added and the resulting slurry was stirred for several hours to obtain homogeneity. Subsequently, the homogenized slurry was titrated with aqueous ammonia until pH 8.5. Thus, precipitated gel was filtered, washed several times and dried at 393 K before subjecting to calcination treatment at 723 K for 4 h. A small portion of the above catalyst was further calcined at 873 K for 4 h to evaluate the thermal stability.

2.2. Catalyst characterization

Powder X-ray diffraction (XRD) patterns of various samples were recorded on a Siemens D-5000 diffractometer, using Ni-filtered Cu Kα (0.15418 nm) radiation source. Crystalline phases were identified by comparison with the reference data from International Centre for Diffraction Data (ICDD) files. The BET surface areas were measured by N_2 adsorption using a Micromeritics Gemini 2360 instrument. Prior to analysis, samples were oven dried at 393 K for 12 h and flushed with Argon gas for 2 h. The FT-IR spectra were recorded on a Nicolet 740 FTIR spectrometer at ambient conditions, using KBr disks, with a normal resolution of 4 cm^{-1} and averaging 100 spectra. Scanning electron microscopy analyses were carried out with a Jeol JSM 5410 microscope, operating with an accelerating voltage of 15 kV. SEM micrographs were taken after coating by gold sputtering. Elemental analysis was carried out on a Kevex, Sigma KS3 EDX instrument operating at a detector resolution of 137 eV. The DTA–TGA measurements were made on a Mettler Toledo TG-SDTA apparatus. Sample was heated from ambient to 1273 K under nitrogen flow and the heating rate was 10 K min^{-1}.

2.3. Catalyst evaluation

The vapour phase selective hydrogenation of cinnamaldehyde was carried out in a down flow vertical fixed bed differential quartz micro-reactor (i.d. 10 mm) at normal atmospheric pressure. In a typical experiment, ca. 0.3 g of catalyst with twice the amount of quartz was secured between two plugs of quartz wool. Ceramic beads were filled above the catalyst bed, which act as preheating zone. The reactor was placed vertically inside a tubular furnace, which was heated electrically. The reactor temperature was monitored by a k-type thermocouple with its tip located near the catalyst bed and connected to a temperature-indicator-controller. Prior to reaction, the catalyst was pre-reduced in flowing H_2 for 3 h. Cinnamaldehyde was fed (1–3 ml h^{-1}) from a motorized syringe pump (Perfusor Secura FT, Germany) into the vapourizer where it was allowed to mix uniformly with H_2 gas (20 ml min^{-1}) before entering the preheating zone of the reactor. The liquid products collected through spiral condensers in ice-cooled freezing traps were analyzed by a gas chromatograph using SE-30 packed column and FID detector. The activity data were collected under steady-state conditions. The conversion, selectivity, and yield were calculated as per the procedure described elsewhere [25].

3. Results and discussion

The N_2 BET surface areas of various bimetallic catalysts prepared in this investigation and calcined at 723 and 873 K

Table 1
Actual metal loadings, metal loadings from EDX analysis, XRD phases observed, and BET SA measurements of various bimetallic M–M^1/SiO_2 (M = Co, Ni, and Cu; M^1 = Ni, Cu, and Co) catalysts calcined at 723 and 873 K

Calcination temperature (K)	Actual metal loading (wt.%)		Metal loading from EDX analysis (wt.%)		XRD phases	BET SA ($m^2\ g^{-1}$)
	M	M^1	M	M^1		
Co–Ni/SiO_2						
723	10	10	9.8	9.5	$Co_{1.29}Ni_{1.71}O_4$	163
873	–	–	–	–	$Co_{1.29}Ni_{1.71}O_4$	121
Ni–Cu/SiO_2						
723	9.6	10.4	11.1	12.5	NiO; CuO	161
873	–	–	–	–	NiO; CuO	132
Cu–Co/SiO_2						
723	10.38	9.62	11.3	10.4	$Cu_{0.76}Co_{2.24}O_4$	185
873	–	–	–	–	$Cu_{0.76}Co_{2.24}O_4$; CuO	159

are shown in Table 1. As can be noted from Table 1, the 723 K calcined samples exhibit reasonably high specific surface areas. Among the three combinations, the Cu–Co/SiO_2 sample exhibited highest BET SA (185 $m^2\ g^{-1}$). In general, the occurrence of high surface areas can be attributed to the preparation method adopted (deposition–precipitation) and, also, to the use of colloidal silica support. There are certain advantages associated with the use of colloidal silica dispersions. First fact is that the colloidal dispersions are much less reactive towards the deposited catalytic materials. As a consequence, solid-state reactions are less likely to occur with the colloidal materials than with the coprecipitated materials from the soluble salts. Secondly, the particles of the colloids are larger than the particles of the coprecipitated salts. This has a feature of making larger pores and more open structures for the final catalysts. Thus, the coprecipitation of bimetallic precursors along with colloidal silica yielded smaller crystallites of bimetallic oxides on the surface of the SiO_2. However, upon further calcination at slightly higher temperature (873 K) a decrease in the surface area is observed. This decrease in the surface area is due to sintering of the samples.

One of the important objectives in using a support is to achieve an optimal dispersion of the catalytically active components and to stabilize them against sintering. The deposition–precipitation technique takes the advantage of the fact that precipitation onto the carrier needs a lower super saturation than formation of new phases directly from the liquid. The support should, also, be stable under reaction and regeneration conditions and should not adversely interact with solvent, reactants or reaction products. Therefore, colloidal silica support has been employed in the present study. The term colloidal silica refers to a stable, dispersion or sols of discrete nanometric particles of amorphous silica, commonly suspended in water with a size of about 7–12 nm in diameter. Depending on the synthesis conditions, the structure of the colloidal particles may differ from isolated spheroidal particles to agglomerates of complex structures. Colloidal silica exhibits reasonably high specific surface area ranging between 140 and 345 $m^2\ g^{-1}$. The surface area will be typically constant up to the calcination temperature of 873–973 K. However, the porosity is normally lost at tempera-

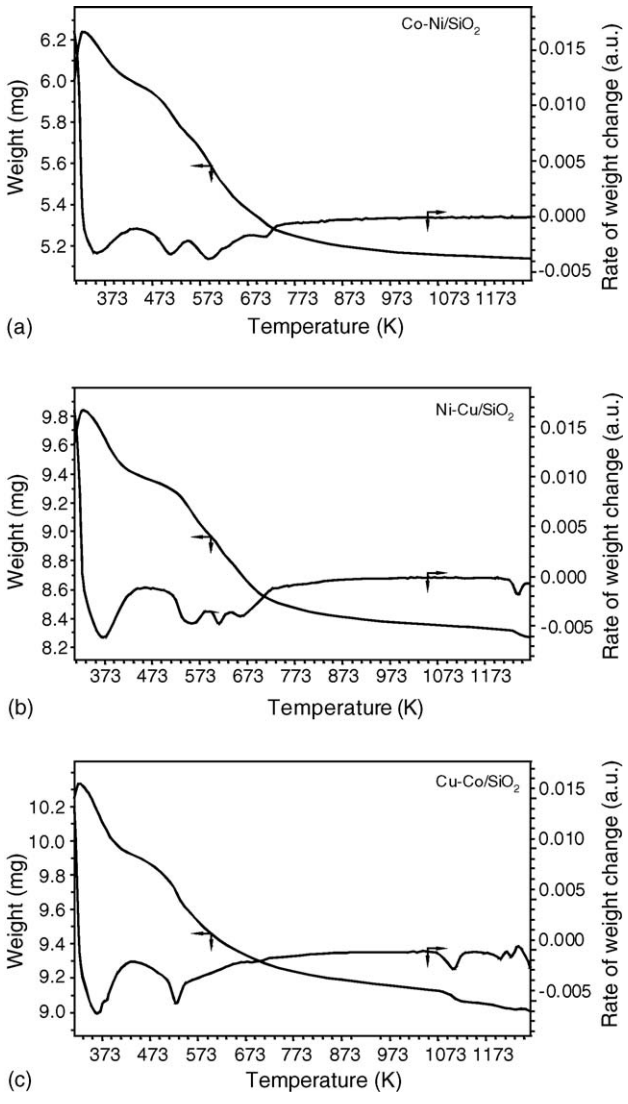

Fig. 1. Thermograms of: (a) Co–Ni/SiO_2, (b) Ni–Cu/SiO_2, and (c) Cu–Co/SiO_2 samples before calcination.

tures higher than 1473 K. Since silica is a neutral oxide, there are no strong Brönsted or Lewis acid or base sites on the surface. Untreated silica is totally hydroxylated and the hydroxyl layer is covered with physically adsorbed water [26]. The physically adsorbed water can be removed by treating at 573 K [26]. Thermal treatment of the supports leads first to removal of water (dehydration) and then to combination of adjacent hydroxyl groups to form water (dehydroxylation). On silica, the dehydroxylation leads to the formation of surface siloxane bridges [27]. To understand the exact behavior of the synthesized bimetallic catalysts on thermal treatment, they were subjected to thermal analysis and dealt in the subsequent paragraph.

The as synthesized bimetallic catalysts were subjected to TG analysis before subjecting them to calcination. The obtained thermograms, recorded in the range ambient to 1273 K and at a ramp of 10 K min^{-1}, are shown in Fig. 1a–c, respectively. As can be observed from Fig. 1a, the thermogram pertaining to Co–Ni/SiO_2 sample exhibits four weight loss peaks in the temperature range 323–773 K. The first major weight loss peak can be attributed to the loss of non-dissociatively adsorbed water as well as water held due to hydrogen bonding. The subsequent weight loss peak is due to the loss of water from the micropores of the hydroxide gel. Loss in weight due to nitrate decomposition and subsequent dehydroxylation could give rise to the other two high temperature peaks. The TG data of the sample revealed a weight loss of 13.1% in four consecutive steps between ambient to 843 K, above which a nominal weight loss of 1.2% is observed until 1273 K. This observation indicates that over the temperature range between 773 and 1273 K, the sample is quite stable in terms of phases and chemical composition.

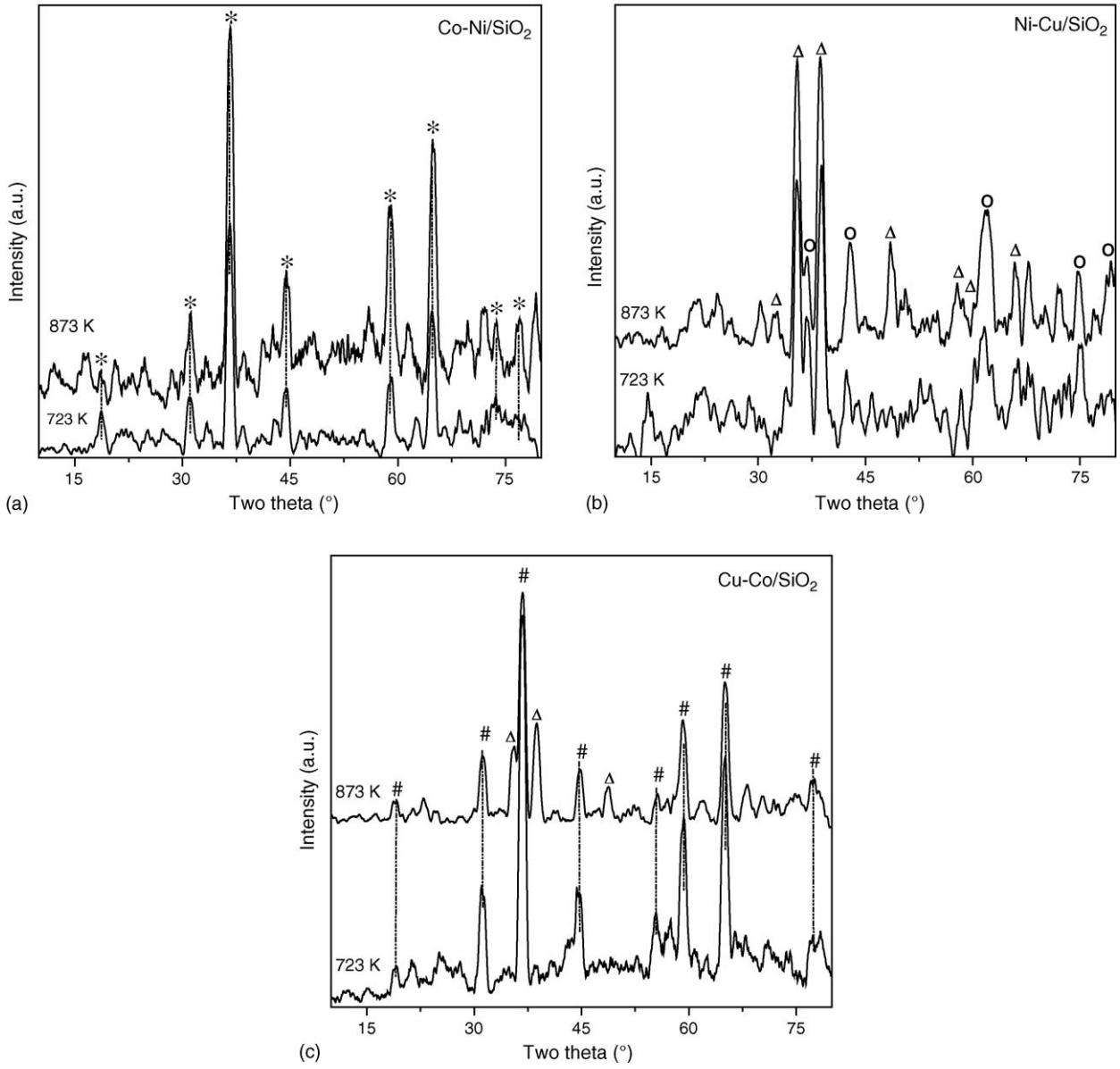

Fig. 2. (a) X-ray powder diffraction patterns of Co–Ni/SiO_2 sample calcined at 723 and 873 K: (*) lines due to $Co_{1.29}Ni_{1.71}O_4$ phase. (b) X-ray powder diffraction patterns of Ni–Cu/SiO_2 sample calcined at 723 and 873 K: (△) lines due to CuO phase; (◯) lines due to NiO phase. (c) X-ray powder diffraction patterns of Cu–Co/SiO_2 sample calcined at 723 and 873 K: (#) lines due to $Cu_{0.76}Co_{2.24}O_4$ phase; (△) lines due to CuO phase.

Fig. 1b represents the TG profile of Ni–Cu/SiO_2 sample. In this case too four weight loss peaks between ambient and 773 K are observed. Similar explanation (as mentioned previously) could be given for the occurrence of these four consecutive peaks. A weight loss of ∼12.2% is observed in the temperature range 313–873 K and above which only 1.62% weight loss could be noted up to 1273 K. Presence of a minor weight loss peak between 1223 and 1273 K could be attributed to loss of copper, which is known to exhibit pyrophoric nature at high temperatures. The thermogram pertaining to Cu–Co/SiO_2 sample (Fig. 1c), also, reveals four weight loss peaks, however, at slightly different temperatures. A weight loss of 1.34% is noted in the temperature range 313–413 K and 2.06% in the 413–513 K range. Between 513 and 1053 K range, the weight loss is 6.15% and a nominal 1.35% weight loss between 1053 and 1273 K. The first-two major weight loss peaks are as usual due to the loss of non-dissociatively adsorbed water and the water held in the micropores of the hydroxide gel. The high temperature weight loss peaks observed above 1073 K could be due to the loss of Cu, as copper is known to be pyrophoric at higher temperatures.

The X-ray powder diffractograms of various samples calcined at 723 and 873 K are presented in Fig. 2a–c, respectively. The oxide mixtures observed either contained segregated phases of NiO (Bunsenite), CuO (tenorite), and CoO (cobalt oxide) or more precisely solid solutions of these combinations. Silica normally exists in any of the three crystallographic forms namely cristobalite, quartz and tridymite. However, no diffraction patterns pertaining to SiO_2 phase could be discerned from XRD results. The non-appearance of SiO_2 diffraction patterns indicates that silica is in highly amorphous state. In general, the XRD patterns of 723 K calcined samples are broad signifying the amorphous nature of the samples. The XRD patterns of Co–Ni/SiO_2 sample (Fig. 2a) reveal the presence of a definite compound between cobalt and nickel with the composition $Co_{1.29}Ni_{1.71}O_4$ (JCPDS 40-1191). With increase in calcination temperature from 723 to 873 K, an increase in the intensity of the peaks pertaining to this phase were noted. This increase in the intensity could be attributed to better crystallization of the sample under high temperature treatment. Fig. 2b shows the XRD patterns of Ni–Cu/SiO_2 sample calcined at 723 and 873 K. As revealed by the diffraction patterns, presence of both CuO (JCPDS 48-1548) and NiO (JCPDS 47-1049)

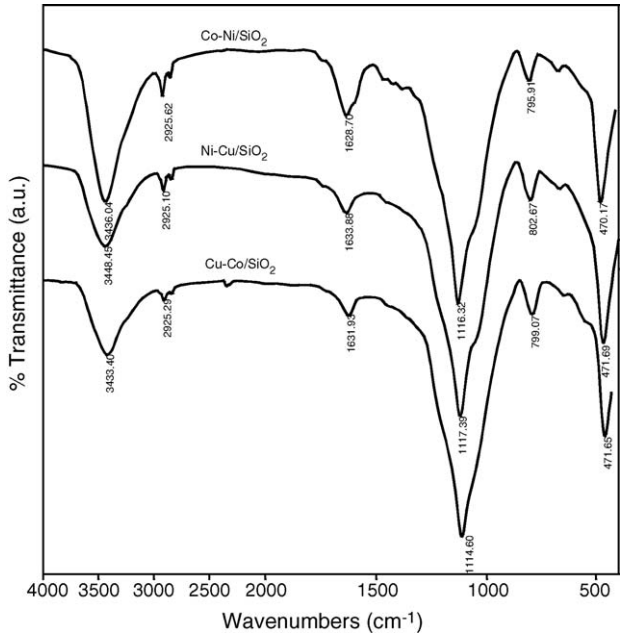

Fig. 3. FT-IR spectra of: (a) Co–Ni/SiO_2, (b) Ni–Cu/SiO_2, and (c) Cu–Co/SiO_2 samples calcined at 723 K.

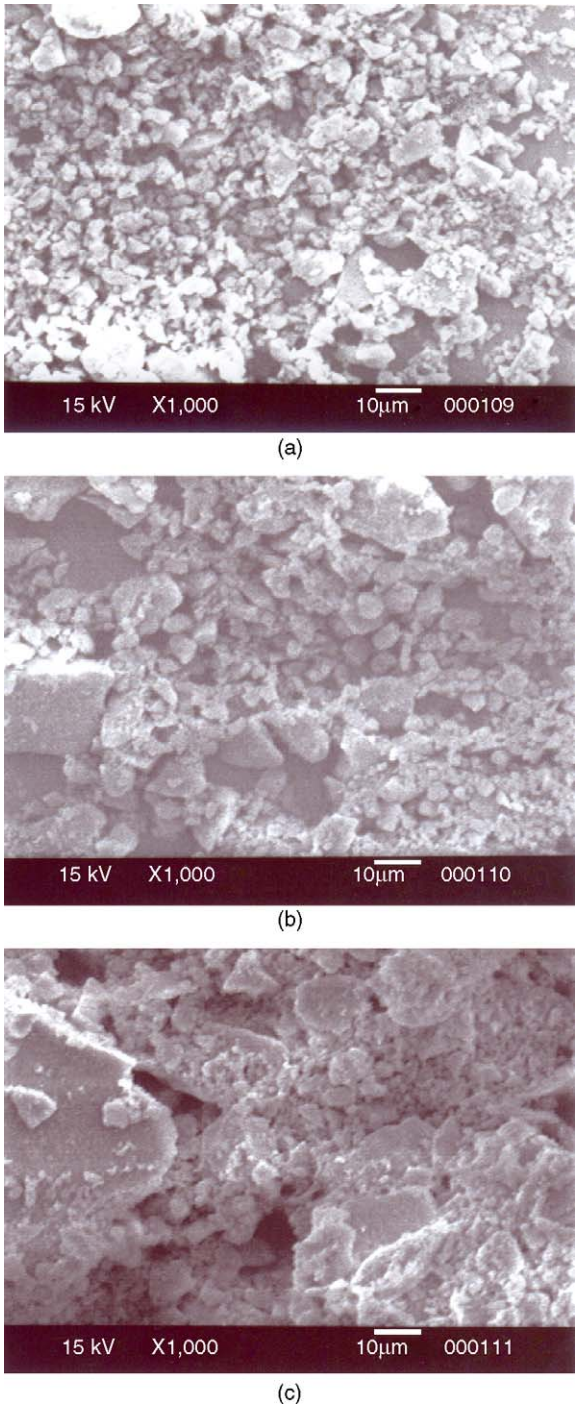

Fig. 4. SEM micrographs of: (a) Co–Ni/SiO_2, (b) Ni–Cu/SiO_2, and (c) Cu–Co/SiO_2 samples calcined at 723 K.

phases could be noted. With increase in calcination temperature, still better crystallized patterns of the above phases are observed. However, as reported by Davies et al. the formation of tetragonal or orthorhombic phases are not observed in the present study due to a different method adopted for the preparation of samples [28,29]. As presented in Fig. 2c, the XRD profiles of Cu–Co/SiO_2 sample calcined at 723 K reveal the formation of a non-stoichiometric cobalt–copper-oxide solid solution $Cu_{0.76}Co_{2.24}O_4$ (JCPDS 36-1189). With increase in calcination temperature from 723 to 873 K, in addition to the $Cu_{0.76}Co_{2.24}O_4$ phase, emergence of crystalline CuO (JCPDS 48-1548) is, also, noted. With increase in calcination temperature, a better crystallization of various phases in the samples is a known phenomenon, which clearly signifies the influence of calcination temperature on the crystallization and formation of new phases in line with literature.

The FT-IR spectra of various bimetallic catalysts recorded in range 4000–400 cm^{-1} are presented in Fig. 3. Strong bands associated with OH stretching vibrations of water and hydroxyl groups occur between 3200 and 3700 cm^{-1}. A strong sharp absorption band in the region 3650–3700 cm^{-1} characterizes the hydroxyl groups. Water of hydration usually exhibits one strong sharp band near 3600 cm^{-1} and one or more strong sharp bands near 3400 cm^{-1}. Water of hydration can be easily distinguished from hydroxyl groups by the presence of the H–O–H bending motion, which produces a medium band in the region 1600–1650 cm^{-1}. Free water has a strong broad absorption band centered in the region 3200–3400 cm^{-1} [30]. Interestingly, all the three bimetallic samples exhibit fairly similar IR patterns, signifying the predominance of silica IR features in the spectra.

To study the surface topography and to assess the surface dispersion of the active components over the SiO_2 substrate, SEM investigation was performed on various samples calcined at 723 K. The obtained representative electron micrographs are presented in Fig. 4a–c, respectively. As estimated from SEM data, the average particle size in the case of Co–Ni/SiO_2 and Ni–Cu/SiO_2 samples is <10 μm and that of Cu–Co/SiO_2 sample is between 10 and 15 μm. Among the various samples studied, the Cu–Co/SiO_2 exhibits more porous texture, hence, was found to exhibit more surface area (Table 1). The energy dispersive X-ray microanalysis (EDX) was, also, performed to get information on the surface composition of various samples. As expected, the EDX results reveal the presence of Si, O, Co, Ni, and Cu elements in the respective samples in appropriate proportions. The amounts of metal loadings detected (wt.%) in the respective samples are presented in Table 1. For the purpose of comparison, the actual metal loadings employed during the preparation are, also, shown in Table 1. The EDX results corroborate well with in the limit of permissible error with the actual metal loadings of the samples.

The catalytic properties of the prepared bimetallic catalysts calcined at 723 K were evaluated for the selective hydrogenation of cinnamaldehyde in the vapour phase. A series of experiments were conducted to determine suitable test conditions for comparison of various catalysts. The activity and selectivity trends were investigated in the temperature range 533–553 K. The activity trends on various bimetallic catalysts followed the same pattern with increasing reaction temperature. In general maximum activity was observed at 543 K, beyond which decomposition of the reactant to produce more undesired products took place.

The activity and selectivity results obtained on various catalysts are shown in Fig. 5. As can be noted from this figure, the Co–Ni/SiO_2 and Ni–Cu/SiO_2 catalysts did not show any selectivity towards the formation of cinnamyl alcohol, however, they exhibited good selectivity towards the formation of hydrocinnamaldehyde (also an important intermediate in the synthesis of HIV drug). Among the three catalysts studied the Cu–Co/SiO_2 combination seems to be active towards the hydrogenation of cinnamaldehyde to cinnamyl alcohol. Further studies are essen-

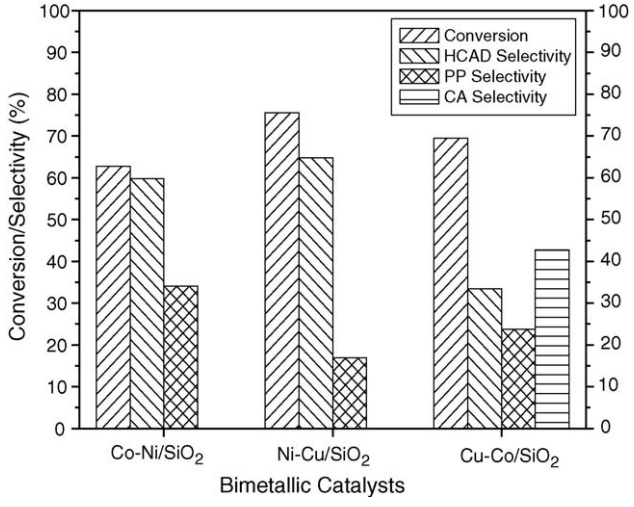

Fig. 5. Conversion and selectivity of Co–Ni/SiO_2, Ni–Cu/SiO_2, and Cu–Co/SiO_2 bimetallic catalysts for selective hydrogenation of cinnamaldehyde: HCAD, hydrocinnamaldehyde; PP, phenyl propanol; CA, cinnamyl alcohol.

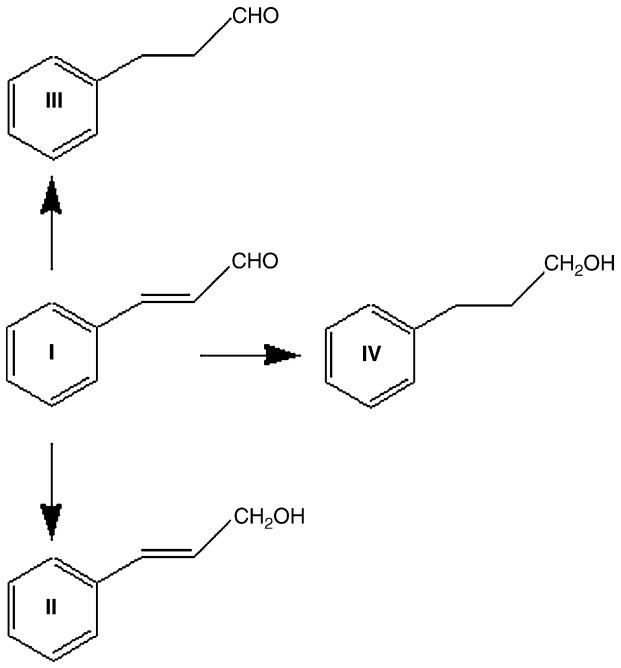

Scheme 1. Reaction scheme of cinnamaldehyde hydrogenation.

tial to investigate the commercial viability of these catalysts for the title reaction. Also, the application of Cu–Co/SiO_2 bimetallic catalysts in the vapour phase could be investigated for other commercially important processes where selective hydrogenation of α,β-unsaturated aldehydes is required.

The hydrogenation of cinnamaldehyde typically produces a mixture of the desired unsaturated alcohol—cinnamyl alcohol, saturated aldehyde—hydrocinnamaldehyde, and the undesired saturated alcohol—phenyl propanol [12,31]. Aldol condensation and other unidentified products were, also, reported in small amounts over particularly non-selective catalysts. The reaction sequence of cinnamaldehyde hydrogenation is illustrated in Scheme 1. Depending on the position of the initial hydrogen addition to the cinnamaldehyde molecule, the carbonyl group and the double bond will be hydrogenated in different series of reactions. Cinnamaldehyde hydrogenation may lead to hydrocinnamaldehyde (III), cinnamyl alcohol (II), and 3-phenyl-1-propanol (IV). In addition, acid-site induced reactions may occur as a result of dehydration reaction of 3-phenyl-1-propanol to β-methyl styrene and isomerisation of hydrocinnamaldehyde to cinnamyl alcohol. According to Delbecq and Sautet [32], as shown in Scheme 2, various adsorption states of the α,β-unsaturated aldehyde are possible on a metal surface. For an adsorption through the C=O double bond, resulting in the formation of cinnamyl alcohol, the geometries are on-top, di-σ_{CO} and π_{CO} (adsorption states a, b and c in Scheme 2). For adsorption through the C=C double bond, resulting in the formation of hydrocinnamaldehyde, the geometries are di-σ_{CC} and π_{CC} (adsorption states d and e). With the quasi-planar (η_4) geometry the adsorption involves both C=C and C=O double bonds (adsorption state f) and results in either the formation of enol as intermediate product or the formation of an unsaturated alcohol, 3-phenyl-1-propanol as the primary product. The enol isomerises to hydrocinnamaldehyde.

The adsorption mode of the α,β-unsaturated aldehyde on a metal surface also depends on the nature of metal and type of exposed crystal face [32]. When the C=C bond is unsubstituted or monosubstituted, the adsorption of α,β-unsaturated aldehyde occurs through both the double bonds in a tetrahepto di-π geometry (adsorption state f in Scheme 2) [32]. Cinnamaldehyde is a monosubstituted molecule with a phenyl ring. When the C=C bond is disubstituted, the di-σ_{CO} geometry (adsorption state b in Scheme 2) is the most stable. This difference in the adsorption can be explained in terms of different radial expansion of 'd' bands of the used metals in the present study as proposed by Anderson [33].

As reported by Gallezot and Richard [3] and Gallezot et al. [34], the amount of allylic alcohol increases with increasing charge density of the active sites. Thus, higher the electron donor strength the stronger is its attack. Accordingly, the charge density of the active sites in the presently investigated samples could be in the order Cu–Co/SiO_2 > Co–Ni/SiO_2 ≅ Ni–Cu/SiO_2. From the present investigation, it is clear that nickel-based catalysts exhibit significant selectivity to hydrocinnamaldehyde and are almost non-selective towards cinnamyl alcohol. The substitution of copper in the place of cobalt increased the activity of Ni-based catalyst, and reduced the formation of undesired phenyl propanol. In the cinnamaldehyde molecule, besides C=C double bond and C=O group, the benzene ring is, also, susceptible to the hydrogenation and hydrogenolysis reactions. However,

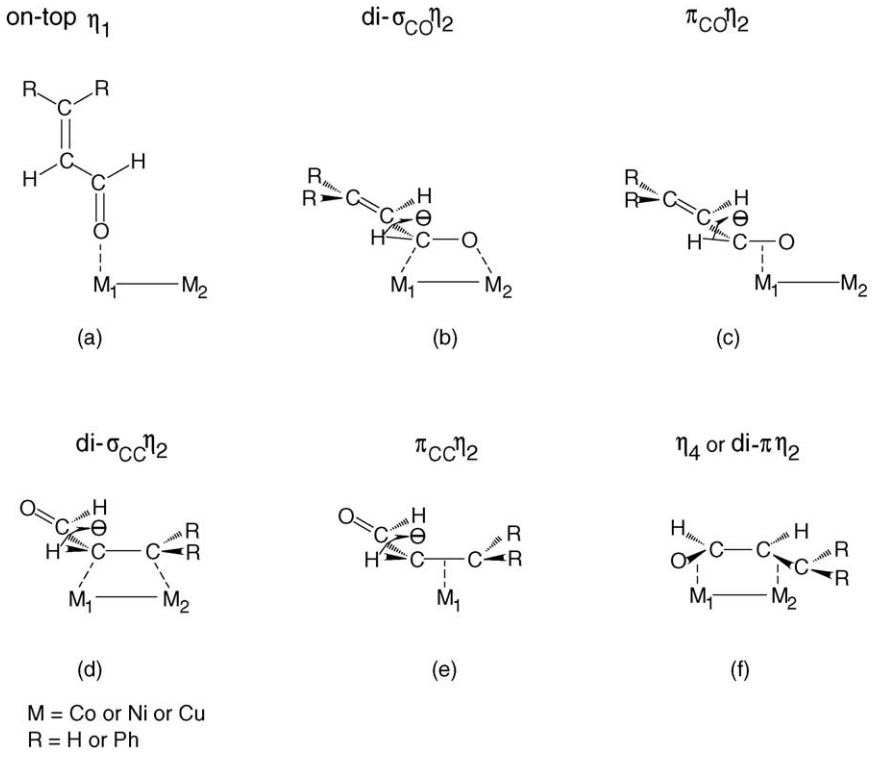

Scheme 2. Adsorption modes of cinnamaldehyde.

such side products were not observed in the present investigation. In the case of Cu–Co/SiO_2 catalysts, the selectivity towards the hydrogenation of the carbonyl bond could be either due to the creation of defect sites at the metal-oxide interface after a high-temperature reduction treatment (773 K), which are able to activate the C=O double bond, or due to electronic effects that may even form Cu–Co alloy phases upon reduction treatment of the $Cu_{0.76}Co_{2.24}O_4$ oxide solid solution.

Finally, a crucial point in catalytic studies over bimetallic systems is the knowledge of the surface composition of the metallic phases. Experimental studies and theoretical calculations suggest indeed that the surface and bulk composition of alloys may differ, making rather difficult the interpretation of alloying effects on the catalytic activities. In principle, one can vary the surface properties of these catalysts in a systematic manner simply by altering the overall metal composition. The composition of bimetallic catalysts is often significantly different at the surface compared to the bulk due to the difference in surface energies of the two metals. The surface composition or the relative fraction of the two metals at the surface is an important parameter in the study of catalytic phenomena. Further studies will be pursued in that direction over these samples.

4. Conclusions

The following conclusions can be drawn from the present study. (i) The Cu–Co/SiO_2, Co–Ni/SiO_2, and Ni–Cu/SiO_2 bimetallic catalysts exhibit interesting catalytic activity for the vapour phase hydrogenation of cinnamaldehyde. (ii) The Cu–Co/SiO_2 combination catalyst exhibits good selectivity towards the formation of cinnamyl alcohol, while the other two systems show selectivity towards the formation of hydrocinnamaldehyde. (iii) Incorporation of silica support in the colloidal form during the coprecipitation of bimetallics results in the stable and well-formed catalysts with high specific surface areas. (iv) Further studies are highly essential to investigate the commercial viability of these catalysts for the selective hydrogenation of cinnamaldehyde to cinnamyl alcohol or hydrocinnamaldehyde, as both of them are very useful products.

Acknowledgements

Authors thank DST, New Delhi for financial support under SERC Scheme (SR/S1/PC-31/2004). AK thanks CSIR, New Delhi for the award of senior research fellowship.

References

[1] M. Bartók, K. Felföldi, in: M. Bartók, et al. (Eds.), Stereochemistry of Heterogeneous Metal Catalysis, Wiley, Chichester, 1985 (Chapter VII); R.L. Augustine, Heterogeneous Catalysis for Synthetic Chemists, Dekker, New York, 1996.
[2] M. Bartók, M. Molnár, in: S. Patai (Ed.), The Chemistry of Double-Bonded Functional Groups, Supplement A3, Wiley, New York, 1997, p. 843.
[3] P. Gallezot, D. Richard, Catal. Rev. Sci. Eng. 40 (1998) 81.
[4] P. Gallezot, A. Giroir-Fendler, D. Richard, in: W.E. Pascoe (Ed.), Catalysis of Organic Reactions, vol. 47, Marcel Dekker, New York, 1992 (Chapter 1).
[5] K. Bauer, D. Garbe, Common Fragrance and Flavor Materials, VCH Publishers, 1985.
[6] J. Kijenski, P. Winiarek, Appl. Catal. A: Gen. 193 (2000) L1.
[7] F. Delbecq, P. Sautet, J. Catal. 152 (1995) 217.
[8] I. Kroschwitz (Ed.), Kirk-Othmer Encyclopedia of Chemical Technology, vol. 6, 4th ed., Wiley, New York, 1992, p. 349.
[9] S. Narayanan, Bull. Cat. Soc. India 2 (2003) 107.
[10] A.M.C.F. Castelijns, J.M. Hogeweg, S.P.J.M. van Nispen, PCT Int. Appl., WO 96/11898 Al (April 25, 1996) 14 pp.; A.M.C.F. Castelijns, J.M. Hogeweg, S.P.J.M. van Nispen, PCT Int. Appl., US Patent 5,811,588 (September 22, 1998) 6 pp.
[11] A. Muller, J. Bowers, WO Patent WO 99/08989 (February 25, 1999) to First Chemical Corporation.
[12] M. Lashdaf, A.O.I. Krause, M. Lindblad, M. Tiitta, T. Venäläinen, Appl. Catal. A: Gen. 241 (2003) 65.
[13] J.P. Breen, R. Burch, J. Gomez-Lopez, K. Griffin, M. Hayes, Appl. Catal. A: Gen. 268 (2004) 267.
[14] J. Hajek, N. Kumar, T. Salmi, D.Y. Murzin, H. Karhu, J. Va1yrynen, L. Cerveny, I. Paseka, Ind. Eng. Chem. Res. 42 (2003) 295.
[15] B. Coq, F. Figueras, Coord. Chem. Rev. 178–180 (1998) 1753.
[16] P. Kluson, L. Cerveny, Appl. Catal. A: Gen. 128 (1995) 13.
[17] U.K. Singh, M.A. Vannice, Appl. Catal. A: Gen. 213 (2001) 1.
[18] J. Hájek, N. Kumar, P. Mäki-Arvela, T. Salmi, D.Y. Murzin, J. Mol. Catal. A: Chem. 217 (2004) 145.
[19] Y. Zhang, S. Liao, Y. Xu, D. Yu, Appl. Catal. A: Gen. 192 (2000) 247.
[20] V. de Jong, M.K. Cieplik, W.A. Reints, F. Fernandez-Reino, R. Louw, J. Catal. 211 (2002) 355.
[21] V. Ponec, Appl. Catal. A: Gen. 222 (2001) 31.
[22] B. Coq, F. Figueras, J. Mol. Catal. A: Chem. 173 (2001) 117.
[23] P. Beccat, J.C. Bertolini, Y. Gauthier, J. Massardier, P. Ruiz, J. Catal. 126 (1990) 451.
[24] T. Birchem, C.M. Pradier, Y. Berthier, J. Cordier, J. Catal. 146 (1994) 503.
[25] B.M. Reddy, I. Ganesh, A. Khan, J. Mol. Catal. A: Chem. 173 (2004) 117.
[26] D.R. Kinney, I.-S. Chuang, G.E. Maciel, J. Am. Chem. Soc. 115 (1993) 6786.
[27] A.A. Tsyganenko, V.N. Filimonov, J. Mol. Struct. 19 (1973) 579.
[28] P.K. Davies, J. Electrochem. Soc. 129 (1982) 31.
[29] J. Bularzik, P.K. Davies, A. Navrotsky, J. Am. Ceram. Soc. 69 (1986) 453.
[30] R.A. Nyquist, L.L. Putzig, M.A. Leugers, Handbook of Infrared and Raman Spectra of Inorganic Compounds and Organic Salts, Academic Press, 1997.
[31] M. Lashdaf, J. Lahtinen, M. Lindblad, T. Venalainen, A.O.I. Krause, Appl. Catal. A: Gen. 276 (2004) 129.
[32] F. Delbecq, P. Sautet, J. Catal. 152 (1995) 217.
[33] J. Anderson, Structure of Metallic Catalysts, Academic Press, New York, 1975, p. 8.
[34] A. Giroir-Fendler, D. Richard, P. Gallezot, Stud. Surf. Sci. Catal. 41 (1998) 171.